9th International Conference on Nano-Molecular Electronics

The effect of backflow on the field-induced director alignment process: Nuclear Magnetic Resonance study and theoretical analysis

Akihiko Sugimura[a], A.A. Vakulenko[b], A.V. Zakharov[b,*]

[a]*Department of Information Systems Engineering, Osaka Sangyo University, 3-1-1 Nakagaito, Daito-Shi, Osaka 574-8530, Japan*
[b]*Saint Petersburg Institute for Machine Sciences, the Russian Academy of Sciences, Saint Petersburg 199178, Russia*

Abstract

The nature of the orientational relaxation process of the director, $\hat{\mathbf{n}}$, to its equilibrium orientation, $\hat{\mathbf{n}}_{eq}(r)$, in a liquid crystal cell has been investigated both experimentally and theoretically. The experiments employ deuterium NMR spectroscopy to investigate the time-resolved field-induced director orientation, and the theory is based on a numerical study of the system of hydrodynamic equations; these include both director motion and fluid flow and take account of backflow. The relaxation time and the influence of the effect of backflow on the orientational relaxation process for a thin nematic film of $4 - n - pentyl - 4' - cyanobiphenyl$ has been investigated for a number of dynamic regimes. Reasonable agreement is observed between the calculated values and experimental results.

Keywords: Liquid Crystals, Anisotropic systems, Nuclear Magnetic Resonance Spectroscopy

1. Introduction

It is important, both from an academic and a technological point of view, to investigate the dynamic director reorientation in a thin nematic liquid crystal film confined between two transparent electrodes and subject to competing constraints. In the presence of external torques and surface anchoring in a nematic film, the motion of the director, $\hat{\mathbf{n}}(r, t)$, to its equilibrium orientation, $\hat{\mathbf{n}}_{eq}(r)$, acting, for instance, under external electric and magnetic fields, is governed by elastic, electric, magnetic, and viscous torques. Taking into account the fact that the nematic phase is especially sensitive to external constraints, there is considerable interest in the director distribution and relaxation in the interior and at the surfaces of a nematic cell. If the director is perturbed, for instance, by means of an electric field, and then allowed to relax, these torques vanish when the director aligns at the equilibrium angle, $\theta_{eq}(r)$, with respect to the normal, $\hat{\mathbf{k}}$, to the cell surfaces. However, any physical effect that reorients the director induces flow in the nematic phase, which, in turn, is coupled to the director. This is the so-called backflow effect [1]. Backflow, while having a subordinate role, has been found to change, qualitatively, the orientational behaviour of the director in its electrically-driven reorientation. To the lowest order, backflow can be considered in a theory by renormalizing the rotational viscosity coefficient, γ_1 [2], but this approach is valid only if the reorientation is small. To high order, backflow can be accounted for by a numerical study of the complete system of hydrodynamic equations that include both

---

*Corresponding author. Tel.: +7-812-321-2470; fax: +7-812-321-4771.
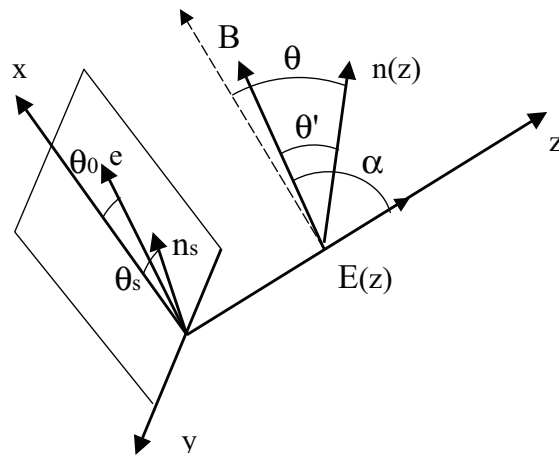*E-mail address*: avz0911@yahoo.com

Figure 1: The geometry used for the time-resolved NMR experiments and the calculations. The z-axis is parallel to the electric field, **E**, and so normal to the electrodes. The magnetic field, **B**, electric field **E**, and director, $\hat{\mathbf{n}}$, are in the xz-plane. The director makes the angle θ with the x-axis, and the electric field makes the angle α with the magnetic field.

director reorientation and the velocity field [3]. So, it should be expected that backflow will also play a crucial role in the reorientational relaxation in nematic films. Recently, time-resolved deuterium nuclear magnetic resonance (NMR) spectroscopic measurements of field-induced director reorientation have been performed [4-7]. Taking into account that the quadrupolar splitting is related to the angle made by the director with the magnetic field, deuterium NMR spectroscopy is found to be a powerful method, with which to investigate the static and dynamic director orientation in nematic films.

We have used deuterium NMR spectroscopy to investigate the director dynamics of specifically deuteriated $4 - \alpha, \alpha - d_2 - pentyl - 4' - cyanobiphenyl$ (5CB-d_2) subject to both magnetic and electric fields in the nematic phase. The electric field is applied at an angle, α, to the magnetic field of the spectrometer (see, Fig.1). This gives a unique reorientation pathway. A sequence of deuterium NMR spectra was acquired as a function of time, which can be used to explore the dynamic director orientation. When the electric field is applied to the nematic film, the director moves from being parallel to the magnetic field to being at an angle to the magnetic field (the turn-on process) because $\Delta\tilde{\epsilon}$ and $\Delta\tilde{\mu}$ are both positive for 5CB. After the electric field is switched off, the director relaxes back to being parallel to the magnetic field (the turn-off process). Deuterium NMR spectra were recorded during the turn-on and the turn-off alignment processes as a function of time. Analysis of these results, based on the predictions of hydrodynamic theory including both the director motion and fluid flow, provides evidence for the importance, or not, of backflow in the relaxation process in the nematic film.

The outline of this paper is as follows. In the next section we describe the NMR experiments and the results obtained. The system of hydrodynamic equations describing both director motion and fluid flow of a nematic film in the cell and the numerical results for a number of relaxation regimes describing both the orientational relaxation of the director and velocity fields as well as the total stress tensor components and torques exerted are given in Sec.3. The discussion of these results and our conclusions are summarized in Sec.4.

2. Experimental details and the results

The nematogen used for this study was 5CB-d_2, specifically deuteriated in the α-position of the pentyl chain. The thin nematic sandwich cell was prepared from glass plates coated with transparent In_2O_3 to act as electrodes; these were not treated in any way. The cell thickness, d, was determined optically and found to be 56.1 μm. The cell was held together by a special glue which is stable in the presence of the cyanobiphenyls and which can be cured using
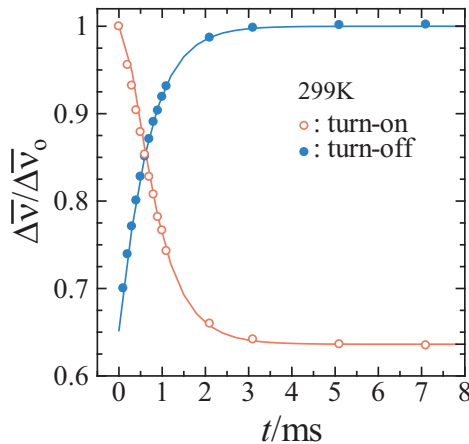
Figure 2: The time dependence of the quadrupolar splitting ratio, $\Delta\tilde{\nu}/\Delta\tilde{\nu}_0$, for the turn-on (open circles) and the turn-off (closed circles) processes determined from the deuterium NMR spectra of 5CB-d$_2$ at 299 K; here the experimental value, $\Delta\tilde{\nu}_0 = 49.6$ kHz has been used to calculate this ratio.

UV radiation for a few minutes. The saturation voltage method [8] was employed to measure the surface anchoring strength, A, at the interface of 5CB-d$_2$ with the substrate surface; it was found to be 10^{-7} Jm^{-2}. This corresponds to a weak anchoring condition and so does not influence the director orientation in the presence of the strong electric and magnetic fields used in our experiments. The measurements were made at 299 K in the nematic phase of 5CB-d$_2$. The spectra were recorded using a JEOL Lambda 300 spectrometer, which has a magnetic flux density, B, of 7.05T. The spectra measured during the turn-on and the turn-off processes were obtained using quadrupolar echo pulse sequences, with a 90° pulse of 7.7 μs and an interpulse delay of 40 μs; the post delay time was 30 ms. The number of free induction decays used to produce spectra with good signal-to-noise varied from 2,000 to 10,000 depending on the sharpness of the spectral lines. The nematic cell was held in the NMR probe head so that the electric field, whose direction is normal to the substrate surface, makes an angle, α, with the magnetic field (see Fig.1). The final adjustment of the cell's orientation to ensure that the electric field makes the desired angle with the magnetic field was carried out by switching on a high electric potential (100 V_{rms}) and rotating the cell by a few degrees, clockwise or counter-clockwise, using an ultrasonic stepping motor until the appropriate doublet splitting was obtained. In that case the quadrupolar splitting is given by [7]

$$\Delta\tilde{\nu}(\theta') = \Delta\tilde{\nu}_0 P_2(\cos\theta'), \qquad (1)$$

where $\Delta\tilde{\nu}_0$ is the splitting when the director is parallel to the magnetic field, $\mathbf{B}$, $P_2(\cos\theta')$ is the second Legendre polynomial and θ is the angle between the director and $\mathbf{B}$. On applying or removing the electric field, the monodomain director orientation is expected to move in the plane defined by $\mathbf{B}$ and $\mathbf{E}$.

   The nematic cell containing 5CB-d$_2$ was held in the NMR probe head so that the electric field makes an angle of about 45° with the magnetic field (see Fig.1). For the turn-on process the director relaxation was monitored at several values of t between 0 and 15 ms following the application of the electric field. For the turn-off process, the director relaxation was measured at values of time in the same range. An electric potential of 50 V_{rms} was applied to obtain the initial director alignment for the turn-off experiments. Deuterium NMR spectra were recorded during the turn-on and turn-off processes [6]. In the turn-on process, the quadrupolar splitting is observed to decrease and then saturates with time corresponding to the equilibrium alignment of the director. Fig.2 shows the temporal variation in the ratio of the quadrupolar splittings, $\Delta\tilde{\nu}/\Delta\tilde{\nu}_0$, determined from the time-resolved deuterium NMR spectra recorded at 299 K for the

turn-on and turn-off processes. We can see that for the turn-on process the director rotates from its initial orientation, $\theta'_0 = 0°$, at which $\Delta\tilde{\nu}_0 = 49.6$ kHz, and then aligns at the limiting angle, θ'_∞ , of 29.5°, determined from Eq.(1) with $\Delta\tilde{\nu}_\infty = 31.5$ kHz, the limiting value of $\Delta\tilde{\nu}(t)$ as t tends to infinity. In the turn-off process, the time dependence of the director orientation was obtained in the same way and is also shown in Fig.2. The time dependence of the director reorientation, described by the angle $\theta'(t)$, has been obtained analytically [7], as

$$\tan\left(\theta'(t) - \theta'_\infty(\alpha)\right) = \tan\left(\theta'_0 - \theta'_\infty(\alpha)\right)\exp\left(-\frac{t}{t_{\mathrm{ON(OFF)}}}\right). \tag{2}$$

Here $\theta'_\infty(\alpha)$ is the limiting value of $\theta'(t)$ when t tends to infinity, θ'_0 is the initial director orientation, and times $t_{\mathrm{ON(OFF)}}$ are related to the material parameters by

$$t_{\mathrm{ON(OFF)}} = \frac{\gamma_1}{\Delta\epsilon_0\epsilon_a E^2}, \tag{3}$$

and

$$\Delta = \left(1 + 2\rho\cos 2\alpha + \rho^2\right)^{\frac{1}{2}}, \tag{4}$$

where $\rho = \mu_0\epsilon_0\left(\frac{E}{B}\right)^2\frac{\epsilon_a}{\chi_a}$, ϵ_a denotes the nematic dielectric anisotropy, χ_a is the anisotropy of the diamagnetic susceptibility of the nematic, and the limiting value θ'_∞ is given by

$$\cos 2\theta'_\infty = -\frac{1 + \rho\cos 2\alpha}{\Delta}. \tag{5}$$

The values of the two times, t_{OFF} and t_{ON}, were obtained by fitting the ratio of the quadrupolar splittings obtained as a function of time for the turn-on and turn-off processes. The solid lines in Fig.2 show the best fits giving the values for t_{ON} and t_{OFF} as 0.594 ms and 1.18 ms, respectively. We have chosen to fit the time dependence of the quadrupolar splitting ratio rather than that for the director orientation calculable from it because the splitting constitutes the primary experimental data and the absolute error associated with each point is more or less constant. An accurate value for the angle between the magnetic and electric fields of 44.7° was calculated by substituting the values of $\Delta\chi/\Delta\epsilon = 1.04 \times 10^{-7}$, $\gamma_1 = 0.0526$ Pa s, $\Delta\epsilon = 10.8$, $B = 7.05$ T, and the value of voltage in 50 V across the nematic film in 56.1 μm thick, for θ'_∞ into Eq.(5).

In order to investigate the monodomain director relaxation subject to both electric and magnetic fields, taking backflow into account, induced by the electric field and the director reorientation, a numerical study of the full system of hydrodynamic equations that include both director reorientation and fluid flow was carried out. To introduce this study we shall now consider the Leslie-Ericksen theory [10,11] for the time dependence of both the director and the velocity fields.

3. Theoretical treatment and numerical results

The coordinate system defined by our experiment assumes that the electric field, $\mathbf{E}(z)$ is applied normal to the electrodes, whereas the magnetic field, $\mathbf{B}$, is applied at an angle α with respect to the electric field (see Fig.1). We consider a nematic system such as cyanobiphenyl, which is confined between two electrodes that impose a preferred orientation of the director, $\hat{\mathbf{n}}(r)$, at the aligning surfaces, for instance, both uniform planar. The coordinate system defined for our task assumes that the director is in the xz-plane (or in the yz-plane), where $\hat{\mathbf{i}}$ is the unit vector directed parallel to the surfaces, which coincides with the planar director orientation on the lower aligning surface, and $\hat{\mathbf{i}}$ is a unit normal vector directed away from the lower substrate to the upper one. Assuming that the electric field, $\mathbf{E}(z) = E(z)\hat{\mathbf{k}}$, varies only in the z-direction, we can suppose that the components of the director, $\hat{\mathbf{n}} = \cos\theta(t,z)\hat{\mathbf{i}} + \sin\theta(t,z)\hat{\mathbf{k}}$ (see Fig.1), as well as other physical quantities, also depend only on the z-coordinate. Here θ denotes the angle between the director and the magnetic field. In the following we deal with the complicated flow, $\mathbf{v}(t,z)$, induced by the electric field and the director reorientation, together with the incompressibility condition and no-slip boundary conditions on the restricted surfaces $\mathbf{v}_{z=0}(z) = \mathbf{v}_{z=d}(z) = 0$, which implies that only one non-zero component of the vector $\mathbf{v}$ exists, viz., $\mathbf{v}(t,z) = v_x(t,z)\hat{\mathbf{i}} = u(t,z)\hat{\mathbf{i}}$. In that case the Navier-Stokes equation reduces to [12,13]

$$\rho\partial_t u(t,z) = \partial_z\sigma_{zx}, \tag{6}$$

$$p_z(t, z) + \frac{\partial \mathcal{R}}{\partial \theta_t} \theta_z = 0, \tag{7}$$

where ρ is the mass density, $\partial_t = \partial/\partial t$, $\partial_z = \partial/\partial z$, $p_z = \frac{\partial p(t,z)}{\partial z}$, and $p(t, z)$ is the hydrostatic pressure in the cell, $\mathcal{R} \equiv \mathcal{R}(\theta, u) = \frac{\gamma_1}{2} \left(h(\theta) u_z^2 + 2\mathcal{A}(\theta) \theta_t u_z + \theta_t^2 \right)$ is the Rayleigh dissipation function, $\mathcal{A}(\theta) = \frac{1}{2} \left(1 + \frac{\gamma_2}{\gamma_1} \cos 2\theta \right)$, $h(\theta) = \frac{1}{\gamma_1} \left(\frac{\alpha_1}{2} \sin^2 2\theta + (\alpha_5 - \alpha_2) \sin^2 \theta + (\alpha_3 + \alpha_6) \cos^2 \theta + \alpha_4 \right)$, $u_z = \frac{\partial u(t,z)}{\partial z}$ is the gradient of the velocity $u(t, z)$, α_i ($i = 1, ..., 6$) are the six Leslie coefficients, and γ_1 and γ_2 are the rotational viscosity coefficients. The stress tensor (ST) component, σ_{zx}, is given by $\sigma_{zx} = \frac{\delta \mathcal{R}}{\delta u_z} = h(\theta) u_z + \mathcal{A}(\theta) \theta_t$, that involves algebraic expressions of the director components and the velocity gradients [12,13]. For the quasi two-dimensional geometry the torque-balance equation describing the reorientation of the nematic film confined between two electrodes can be derived from the balance of elastic, viscous, magnetic, and electric torques $\mathbf{T}_{\text{elast}} + \mathbf{T}_{\text{vis}} + \mathbf{T}_{\text{mag}} + \mathbf{T}_{\text{el}} = 0$, and takes the dimensionless or scaled form [12,13]

$$\theta_\tau = -\mathcal{A}(\theta) u_z + \delta_1 \left(\frac{1}{2} G_\theta(\theta) \theta_z^2 + G(\theta) \theta_{zz} \right) + \frac{\overline{E}^2(z)}{2} \sin 2\theta + \delta_2 \sin 2(\theta + \alpha), \tag{8}$$

where $G(\theta) = \cos^2 \theta + \frac{K_3}{K_1} \sin^2 \theta$, $\theta_{zz} = \partial^2/\partial z^2$, and K_1 and K_3 are the splay and bend elastic constants. Here $\tau = \left(\frac{\Delta \epsilon \epsilon_0 E^2}{\gamma_1} \right) t$ and $\overline{z} = \frac{z}{d}$ are the scaled time and scaled distance from the bottom electrode, d is the thickness of the cell, $\Delta \epsilon = \epsilon_\parallel - \epsilon_\perp$, $\epsilon_\parallel$ and $\epsilon_\perp$ are the dielectric constants parallel and perpendicular to the director, while $\delta_1 = \frac{K_1}{\Delta \epsilon \epsilon_0 E^2 d^2}$ and $\delta_2 = \frac{\Delta \chi B^2}{2\Delta \epsilon \epsilon_0 E^2 \mu_0}$ are two parameters for the system. Notice that the overbars in the space variable z have been (and will be) eliminated in the last as well as in the following equations. The application of the voltage across the nematic film results in a variation of $E(z)$ through the film [5-7] which is obtained from

$$\frac{\partial}{\partial z} \left[\left(\frac{\epsilon_\perp}{\Delta \epsilon} + \sin^2 \theta(\tau, z) \right) \overline{E}(z) \right] = 0,$$

$$1 = \int_0^1 \overline{E}(z) dz, \tag{9}$$

where $\overline{E}(z) = \frac{E(z)}{E}$, $E = \frac{U}{d}$, and U is the voltage applied across the cell. To be able to observe the evolution of the angle $\theta(\tau, z)$ to its equilibrium value, $\theta_{\text{eq}}(z)$, the evolution of the velocity field, $u(\tau, z)$, caused both by the electric field and the director reorientation to its equilibrium orientation, we consider also the scaled analog of the Navier-Stokes (see Eq.(6))

$$\delta_3 \partial_\tau u(\tau, z) = \partial_z \sigma_{zx}, \tag{10}$$

where $\delta_3 = \rho \epsilon_0 \Delta \epsilon \left(\frac{Ed}{\gamma_1} \right)^2$ is an additional characteristic parameter for the system. Note that the overbars in the electric field $\overline{E}(z)$ will be removed in the following equations. Consider now the nematic film between the two electrodes when the director is weakly anchored at the surfaces and the anchoring energy takes the form [9] $W = \frac{1}{2} A \sin^2 (\theta_s - \theta_0)$, where θ_s and θ_0 are the angles corresponding to the director orientation on the solid surface, $\hat{\mathbf{n}}_s$, and easy axis, $\hat{\mathbf{e}}$, respectively. The torque balance transmitted to the surfaces assumes that the director angle has to satisfy the boundary conditions [12]

$$G(\theta) (\partial \theta(z)/\partial z)_{z=0} = \frac{Ad}{2K_1} \sin 2\Delta\theta^-, \, G(\theta) (\partial \theta(z)/\partial z)_{z=1} = \frac{Ad}{2K_1} \sin 2\Delta\theta^+, \tag{11}$$

where $\Delta\theta^\pm = \theta_s^\pm - \theta_0^\pm$, whereas the initial orientation of the director is directed parallel to both surfaces, with $\theta(\tau = 0, z) = 0$, and then allowed to relax to its equilibrium value $\theta_{\text{eq}}(z)$ Here $\theta_s^\pm$ and $\theta_0^\pm$ are the pretilt angles of the surface director and the easy axes at $z = 0$ and $z = 1$, respectively. The no-slip condition on $\mathbf{v}$ at both solid surfaces assumes that the velocity has to satisfy the boundary conditions [12,13]

$$u(z)_{z=0} \equiv v_x(z)_{z=0} = 0,$$

$$u(z)_{z=1} \equiv v_x(z)_{z=1} = 0. \tag{12}$$

Now the reorientation of the director in the nematic film between the two solid surfaces, when the relaxation regime is governed by the viscous, elastic, magnetic, and electric torques, and including backflow, can be obtained by solving
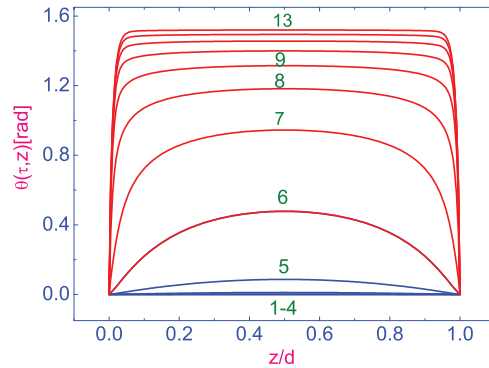
Figure 3: The evolution of the angle $\theta(\tau, z)$, where $\tau = \left(\frac{\Delta \epsilon \epsilon_0 E^2}{\gamma_1}\right) t$ is the scaled time, calculated using Eqs.(8)-(10), with the boundary condition $\left(\frac{Ad}{2K_1} \sin 2\Delta\theta^{\pm} = 0.033\right)$ on both surfaces, taking backflow into account. The first thirteen curves $\theta(\tau, z)$ are plotted as solid lines and neighbouring lines are separated by the time interval $\Delta\tau = 1.0$ up to $\tau = 13$. Here $\alpha = \frac{\pi}{2}$.

the system of non-linear partial differential equations (8)-(10), with appropriate boundary and initial $\theta(\tau = 0, z) = 0$ conditions, both for the angle $\theta(\tau, z)$ (see Eq.(11)) and the velocity $u(\tau, z)$ (see Eq.(12)).

For the case of 5CB, at a temperature of 299 K and density of 10^3 kg/m^3, the measured data for the elastic constants are $K_1 = 9.5$ pN and $K_3 = 13.8$ pN [14], whereas the experimental value for A was found to be 10^7 Jm^{-2} [7]. In the following we use the measured dielectric constants [15] $\epsilon_{\parallel}$ and $\epsilon_{\perp}$, as well as the measured values [7] $\gamma_1 \approx 0.072$ Pas and $\gamma_2 \approx -0.079$ Pas, at 299 K. At 299 K and a density of 10^3 kg/m^3, the values of the six Leslie coefficients were found to be [16]; $\alpha_1 \approx -0.0066$ Pas, $\alpha_2 \approx -0.075$ Pas, $\alpha_3 \approx -0.0035$ Pas, $\alpha_4 \approx 0.072$ Pas, $\alpha_5 \approx 0.048$ Pas, and $\alpha_6 \approx -0.03$ Pas. The value of the voltage across the nematic film, which is 56.1 μm thick, was chosen to be 50 V, as in the experiment. In the case of planar alignment, when the angles θ_s and θ_0 are both close to 0, $\Delta\theta$ is rather small, $\Delta\theta^{\pm} \approx 0.5 - 0.3°$, and therefore $\sin 2\Delta\theta^{\pm} \approx 2\Delta\theta^{\pm}$, consequently the combination of $\left(\frac{Ad}{2K_1} \sin 2\Delta\theta^{\pm}\right)$ values varies between 0.03 and 4×10^{-4}. The set of δ-parameters, which is involved in Eqs.(8)-(10) take the values $\delta_1 \approx 0.53$, $\delta_2 \approx 0.28$ and $\delta_3 \approx 10^{-5}$. Using the fact that $\delta_3 \ll 1$, the Navier-Stokes equation (10) takes the form [12,13]

$$\sigma_{zx} = h(\theta) u_z + \mathcal{A}(\theta) \theta_\tau = C(\tau), \tag{13}$$

where $C(\tau)$ is a function that does not depend on z and is fixed by the boundary conditions. The relaxation of the director to its equilibrium orientation, which is described by the angle $\theta(\tau, z)$, from its initial condition $\theta(\tau = 0, z)$ to $\theta_{eq}(z)$, at the different times ($\tau = 0.0$ (curve(1)),$\tau=13$ (curve (13))) have been investigated with a standard numerical relaxation method [17], with the value $\frac{Ad}{2K_1} \sin 2\Delta\theta^{\pm} = 0.033$, and the results are shown in Fig.3. In this case the effect of backflow on the relaxation process for the angle $\theta(\tau, z)$ in the nematic film is shown. The relaxation criteria $\epsilon = |(\theta_{(m+1)}(\tau, z) - \theta_{(m)}(\tau, z))/\theta_{(m)}(\tau, z)|$ for calculating procedure was chosen equal to be 10^{-4}, and the numerical procedure was then carried out, during the time τ_R, until a prescribed accuracy was achieved. Here τ_R is the relaxation time of the director to its equilibrium orientation. The velocity field $u(\tau, z)$ induced by the director reorientation to its equilibrium orientation relaxes with time to zero; the results of the calculations are shown in Fig.4 (during the set of results up to $\tau = 13$).

For 5CB between the two electrodes with a voltage across the sample of 50 V, both relaxation regimes, that is with and without taking backflow into account, are characterized by a monotonic increase of the angle $\theta(\tau, z)$ up to the equilibrium value $\theta_{eq}(z)$ with, practically, the same relaxation time (see, for instance, Fig.5, where the scaled distance from the bottom electrode is equal to 0.25). Physically, this means that the electric field produces an alignment of the
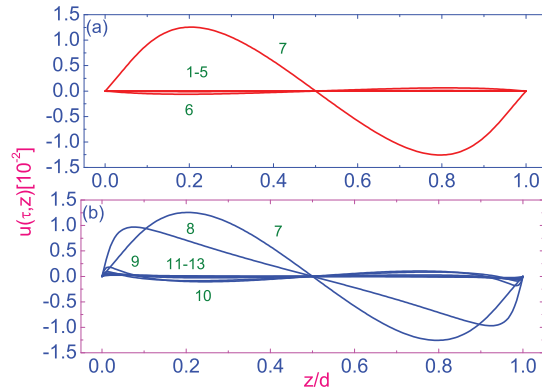
Figure 4: Plot of the evolution of the scaled velocity $u(\tau,z)$ $\left(u \equiv \left(\frac{\gamma_1}{\epsilon_0 \Delta \epsilon E^2 d}\right) v_x\right)$ across the nematic cell, calculated using Eqs.(8)-(10), with the boundary condition $\frac{Ad}{2K_1} \sin 2\Delta\theta^{\pm} = 0.033$. The first thirteen curves $\theta(\tau,z)$ are plotted as solid lines with neighbouring lines separated in time by $\Delta\tau = 1.0$ up to τ of 13. Here $\alpha = \frac{\pi}{2}$.
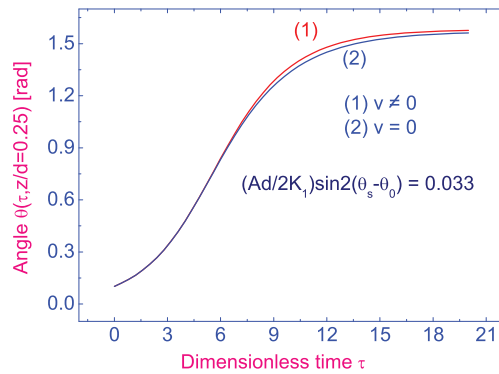

Figure 5: The time dependence of the angle $\theta(\tau,z)$ to its equilibrium value $\theta_{\mathrm{eq}}(z)$, at the dimensionless distance, z, from the bottom electrode of 0.25, both with (curve (1)) and without (curve (2)) taking backflow into account. Here $\alpha = \frac{\pi}{2}$.
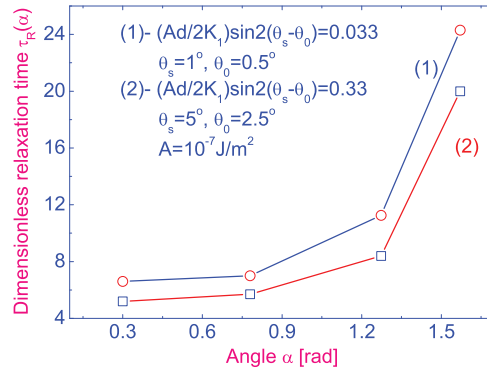
Figure 6: The influence of the angle α between the electric and magnetic fields, and the surface angles θ_s and θ_0 on the scaled relaxation time, $\tau_R(\alpha)$, of the director to its equilibrium orientation.

director away from the magnetic field, caused by applied voltage and that the field has a strong influence, at least in our case, compared with the other torques, on the relaxation process. Our calculations reveal the weak effect of backflow on the relaxation process in the nematic cell under the influence of the electric field. The calculations also show that the electric, magnetic, elastic, and viscous torques exerted are vanishingly small for the case when the electric field is almost orthogonal to the magnetic field after a scaled relaxation time of 20 which corresponds a relaxation time of 18 ms. Calculations also show that the angle between the two fields, α, has a strong influence on the relaxation process for the turn-on regime (see Fig.6). These calculations have been performed for two values of the angle $\Delta\theta$ from 2.5° to 0.5°, at the surface; the scaled relaxation time τ_R increases by up to 20%.

The relaxation process of the velocity field $u(\tau, z)$ in the nematic film between the two electrodes is characterized by an oscillating behavior of $u(\tau, z)$ with change of the scaled distance, z, but with gradual decrease in time, the range of these oscillations decreases, and finally $u(\tau, z)$ adopts a smoother character (see Fig.4), before reaching a zero value. The absolute magnitude of the velocity field $v_x(t, z) = \left(\frac{\epsilon_0 \epsilon_a E^2 d}{\gamma_1}\right) u(t, z)$ in the nematic film between the two electrodes is equal to 0.9 mm/s at the initial stage of the relaxation process (see, for instance, curve (7), of Fig.4). We note that the velocity meets the required boundary conditions (see Eq.(12)), on both electrodes.

Our attention now turns to the stress tensor, σ_{ij}, which can also be obtained directly from the scaled Rayleigh dissipation function $\mathcal{R} = \left(\frac{K_1^2}{\gamma_1 d^4}\right)\overline{\mathcal{R}}$ as [12,18]

$$\sigma_{zx}(\tau) = \frac{\partial \overline{\mathcal{R}}}{\partial u_z}. \tag{14}$$

Having obtained σ_{zx}, we can calculate, from the relation $\sigma_{zx}(\tau) - \sigma_{xz}(\tau) = \frac{\partial \overline{\mathcal{R}}}{\partial \theta_\tau}$, the scaled stress tensor component σ_{xz}. It takes the form [12]

$$\sigma_{xz}(\tau) = C(\tau) - \frac{1}{2}E^2(z)\sin 2\theta - \delta_2 \sin 2(\alpha + \theta) - \delta_1\left[\frac{1}{2}\mathcal{G}_\theta(\theta)\theta_z^2 + \mathcal{G}(\theta)\theta_{zz}\right]. \tag{15}$$

It is important to point out that the balance of linear momentum for $i = z$ (see Eq.(6)), and the viscous contribution, $p(z) = -\int_0^z (\theta_\tau + \mathcal{A}(\theta)u_z)\theta_z dz$, to the arbitrary pressure allows us to derive the remaining components of the scaled stress tensor $\sigma_{zz}(\tau)$ and $\sigma_{xx}(\tau)$ as

$$\sigma_{zz}(\tau) = -E^2(z)\left(\frac{\epsilon_\perp}{\epsilon_a} + \sin^2 \theta\right), \tag{16}$$

$$\sigma_{xx}(\tau) = \sigma_{zz}(\tau) + \delta_1 \mathcal{G}(\theta)\theta_z^2. \tag{17}$$
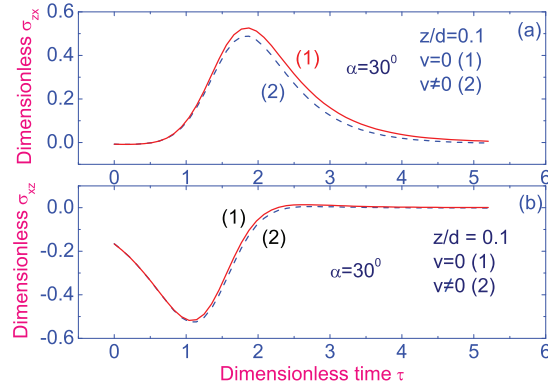
Figure 7: Plot showing the relaxation of the scaled stress tensor components $\sigma_{zx}(z, \tau)$ (a) and $\sigma_{xz}(z, \tau)$ (b) to their equilibrium values, for a 5CB film between two electrodes, at a scaled distance z of 0.1, both without (curve (1)) and with (curve (2)) taking backflow into account. Here $\alpha = \frac{\pi}{6}$.

Having obtained both the angle $\theta(\tau, z)$ and scaled velocity $u(\tau, z)$ we can calculate the components of the scaled stress tensor $\sigma_{ij}(\tau)$ (i, j = x, z). The relaxation of the stress tensor components $\sigma_{zx}(z, \tau)$, $\sigma_{xz}(z, \tau)$, $\sigma_{zz}(z, \tau)$, and $\sigma_{zz}(z, \tau)$ in the nematic film, with and without taking backflow into account, during the scaled time τ up to $\tau \approx 5$ (4.5 ms) are shown in Figs.7 and 8. Calculations of the absolute magnitude of $\overline{\sigma}_{ii} = \left(\epsilon_a \epsilon_0 E^2\right) \sigma_{ii}$ (i = x, z) shows that under the influence of the torques exerted by the component of the stress tensor σ_{zx} is characterized by an increase of $|\overline{\sigma}_{zx}|$ by up to 0.04 Pa within the initial stage of the relaxation process ($\Delta\tau_{zx} \sim 2$) (1.8 ms) (Fig.7(a)), and a fast decrease in $|\overline{\sigma}_{zx}|$ down to zero, within the last stage of the relaxation process. Figs.7 (a) and (b) show that the scaled component of the stress tensor $\sigma_{xz}(\tau, z)$ relaxed to zero twice as fast as the component $\sigma_{zx}(\tau, z)$, whereas both components $\sigma_{xx}(\tau, z)$ and $\sigma_{zz}(\tau, z)$ relaxed to a value of -1.4 (see, Figs.8 (a) and (b)), practically, with the same scaled relaxation time $\Delta\tau_{xx} \sim \Delta\tau_{zz} \sim 5$ (~ 4.5 ms). Also these figures show that at high values of the voltage applied across the LC sample (50 V), there is only a weak effect of the backflow on both the relaxation process of the director field and the stress tensor components. At the same time our calculations show that the relative orientation of the electric and magnetic fields, measured by the angle α has a strong influence on the magnitude and character of the relaxation process of the stress tensor components σ_{zx}, σ_{xz}, σ_{zz}, and σ_{xx} (see Figs. 9 and 10).

On increasing α from 0 to $\frac{\pi}{2}$, the relaxation time $\Delta\tau_{zx}$ for the shear component σ_{zx} increases by a factor of approximately three compared with the relaxation time $\Delta\tau_{xz}$ for the shear component σ_{xz}, from $\Delta\tau_{zx}(0) \approx 6$ (5.4 ms) up to $\Delta\tau_{zx}(\frac{\pi}{2}) \approx 18$ (16.2 ms), and from $\Delta\tau_{xz}(0) \approx 3$ (2.7 ms) up to $\Delta\tau_{xz}(\frac{\pi}{2}) \approx 12$ (11 ms). The same situation holds for the remaining stress tensor components σ_{zz} and σ_{xx} (see Fig. 10 (a) and (b)). Indeed, both at $\alpha = 0°$ and $44.7°$, the magnitude of the scaled stress tensor components σ_{zz} and σ_{xx} relax to their equilibrium values with, practically, the same scaled time $\Delta\tau_{ii}(\alpha) \approx 5$ (4.5 ms), whereas with increase of α of up to $\frac{\pi}{2}$, the magnitude of the scaled components $\sigma_{ii}\left(\frac{\pi}{2}\right)$ (i = x, z) are relaxed over a time which is approximately four times longer $\Delta\tau_{ii}(\frac{\pi}{2}) \approx 20$ (18 ms).

In an attempt to bring the theory and experiment closer we have performed a numerical study of the shear viscosity coefficient [14] $\eta_s \equiv \eta_{zx} = \frac{\sigma_{zx}(\tau, z)}{u_z}$ or

$$\eta_s = h(\theta) + \mathcal{A}(\theta)\frac{\theta_\tau}{u_z}. \tag{18}$$

The relaxation of the scaled viscosity $\frac{\eta_s}{\gamma_1}$ to its equilibrium value in the nematic film of 5CB between two electrodes, with voltage across the sample of 50 V at two different scaled distances of 0.1 (close to the bottom electrode) and 0.5 (in the middle of the film) are shown in Figs.11 (a) and (b). The results in Fig.11 show that the shear viscosity, $\eta_s(\tau)$, relaxes to $\lim_{\tau \to \Delta\tau_s} \eta_s(\tau) \to \eta_s(\text{eq}) \sim 1.4\gamma_1$, practically with the same relaxation time $\Delta\tau_s \sim 9$ (~ 8ms), over the entire thickness of the nematic film. Based on that result one can conclude that the equilibrium value of η_s is equal to $1.4\gamma_1$, and does not depends on α.
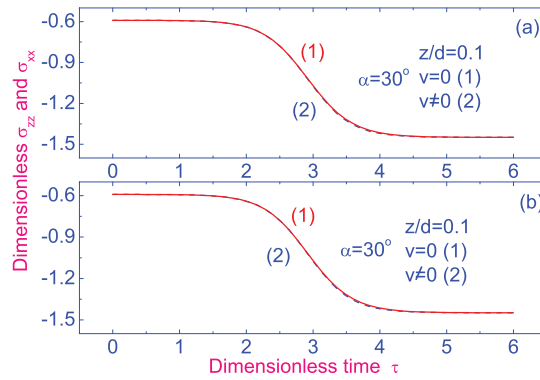
Figure 8: Plot showing the relaxation of the scaled stress tensor components $\sigma_{xx}(z, \tau)$ (a) and $\sigma_{zz}(z, \tau)$ (b) to their equilibrium values, for a 5CB film between two electrodes, at a scaled distance z of 0.1, both without (curve (1)) and with (curve (2)) taking backflow into account. Here $\alpha = \frac{\pi}{6}$.
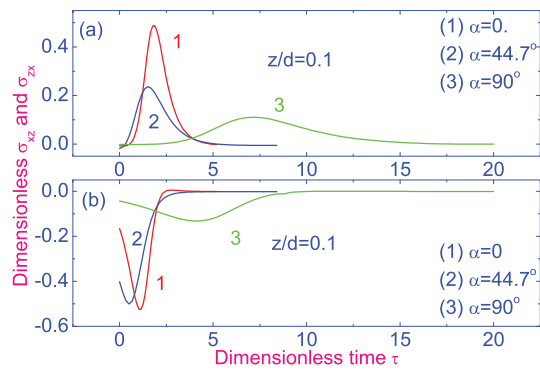

Figure 9: The dependence on the angle α of the shear stress tensor components σ_{zx} (a) and σ_{xz} (b), during relaxation to their equilibrium values, for a 5CB film between two electrodes, at a scaled distance, z of 0.1 from the lower surface taking backflow into account.
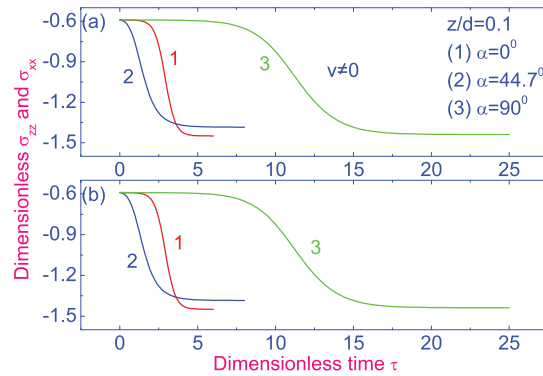
Figure 10: The same as in Fig.9, but showing the relaxation of the scaled normal stress tensor components $\sigma_{xx}(z, \tau)$ (a) and $\sigma_{zz}(z, \tau)$ (b) to their equilibrium values.
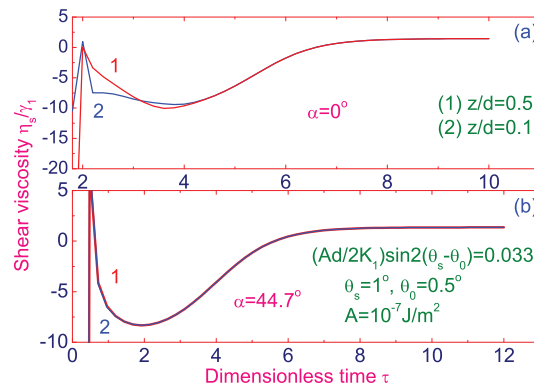

Figure 11: Plot of relaxation of the scaled shear viscosity $\frac{\eta_s}{\gamma_1}$ to its equilibrium value, at two scaled distances, z, of 0.5 (curve (1)) and 0.1 (curve (2)) away from the bottom electrode. The evolution is given at two values of the angle between **E** and **B**, $\alpha = 0$ (a) and 44.7° (b).
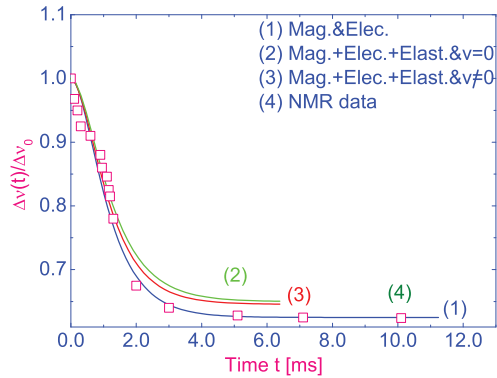
Figure 12: The time dependence of the ratio $\Delta\tilde{\nu}(t)/\Delta\tilde{\nu}_0$ for the turn-on process calculated with accounting for only the electric and magnetic fields (curve (1)), and with (curve (3)) and without (curve (2)) accounting for the backflow effect. The measured Duterium NMR data (values (4)) is obtained for 5CB-d_2 in the nematic phase at 299 K.

4. Discussion and Conclusions

Having obtained the shifted angle, $\theta = \frac{\pi}{2} - \alpha + \theta'$, we can calculate the quadrupolar splitting ratio, $\Delta\tilde{\nu}(t)/\Delta\tilde{\nu}_0 = P_2(\theta'(t))$, determined from the time-resolved deuterium NMR spectra, for instance, for the turn-on process. The evolution of the ratio $\Delta\tilde{\nu}(t)/\Delta\tilde{\nu}_0$ with time, calculated with (curve (3)) and without (curve (2)) taking backflow into account is shown in Fig.12. The time evolution of $\Delta\tilde{\nu}(t)/\Delta\tilde{\nu}_0$ calculated with only the magnetic and electric torques (see, Eq.(2)) is shown in Fig.12 as curve (1). We can see in Fig.12 (curve (1) for the turn-on process that using only the magnetic and electric torques, the director rotates from the initial angle $\theta'_0 = 0°$, and then aligns at the limiting angle $\theta'_\infty(\alpha \sim \frac{\pi}{4}) = 29.8°$. The curves (2) and (3) in Fig.12 show that the director rotates from the initial angle $\theta'_0 = 0°$, under the influence of the voltage (50 V) across the LC sample, which made an angle of 44.7° with the magnetic field ($B = 7.05$ T), and then aligns at the limiting angle $\theta'_\infty(\alpha \sim \frac{\pi}{4}) = 29.8°$, both for the cases when backflow is and is not taken into account. Both these processes are characterized by, practically, the same relaxation time of $\tau_{ON} \approx 7$ ms. This value for τ_{ON} shows that at the high electric and magnetic fields employed in the NMR experiments, the effect of backflow is weak both on the director relaxation and consequently the quadrupolar splitting ratio. At the same time, our calculations show that accounting for the elastic torque, anchoring effect, and backflow leads to a small decrease of the limiting angle $\theta'_\infty(\alpha)$ by about one degree. Reasonable agreement is observed between the calculated values and experimental results.

In summary, we have investigated the the field-induced relaxation of the director $\hat{\mathbf{n}}_{eq}(r)$, velocity $\mathbf{v}(t, z)$ fields, and a number of components of the stress tensor $\sigma_{ij}(\tau)$ $(i, j = x, z)$ to their equilibrium values in a $4 - n - pentyl - 4' - cyanobiphenyl$ nematic film, between two electrodes following the application of a voltage across the sample. Our simulations, in the framework of the classical Ericksen-Leslie theory, suggest that to describe the dynamical reorientation of the director correctly, under the influence of a strong electric field, we do not to need to include a proper treatment of backflow. This means that the role of the magnetic, viscous, and elastic forces becomes negligible in comparison to the electric contribution. In the case of weak magnetic and electric fields, when the role of viscous and elastic forces is increased, backflow must be accounted for by a numerical study of the full system of the hydrodynamic equations that include both the director reorientation and the velocity flow. A balance between the electric, magnetic, elastic, and viscous torques exerted on the director is reflected in the relaxation of the director to its equilibrium position to be determined at an angle $\theta'_\infty(\alpha)$ with respect to the electrodes. We believe that the present investigation has shed some light on the problem of the reorientation processes in nematic films confined between two electrodes, induced by both electric and magnetic fields.

5. Acknowledgment

References

[1] A. Buka and L. Kramer, Pattern Formation in Liquid Crystals, Springer, Berlin, 1995.
[2] A. F. Martins, P. Esnault, F. Volino, Phys. Rev. Lett. 57, 1745 (1986).
[3] G. Demeter, D. O. Krimer, and L. Kramer, Phys. Rev. E72, 051712 (2005).
[4] S. M. Fan, G. R. Luckhurst, and S. J. Picken, J. Chem. Phys. 101, 3255 (1994).
[5] G. R. Luckhurst, T. Miyamoto, A. Sugimura, T. Takashiro, and B. A. Timimi, J. Chem. Phys. 114, 10493 (2001).
[6] G. R. Luckhurst, T. Miyamoto, A. Sugimura, and B. A. Timimi, J. Chem. Phys. 117, 5899 (2002).
[7] G. R. Luckhurst, A. Sugimura, B. A. Timimi, and H. Zimmermann, Liq. Cryst. 32, 1389 (2005).
[8] A. Sugimura, T. Miyamoto, M. Tsuji, and M. Kruze, Appl. Phys. Lett. 72, 329 (1998).
[9] P. G. de Gennes and J. Prost, The Physics of Liquid Crystals, 2nd Ed. Oxford University Press, Oxford, 1995.
[10] J. L. Ericksen, Arch. Ration. Mech. Anal. 4, 231 (1960).
[11] F. M. Leslie, Arch. Ration. Mech. Anal. 28, 265 (1968).
[12] A. V. Zakharov and A. A. Vakulenko, J. Chem. Phys. 127, 084907 (2007).
[13] A. V. Zakharov, A. A. Vakulenko, and S. Romano, J. Chem. Phys. 132, 094901 (2010).
[14] P. P. Karat and N. V. Madhusudana, Mol. Cryst. Liq. Cryst. 40, 239 (1977)
[15] J. Jadzyn, S. Czerkas, G. Czechowski, A. Burczyk, and R. Dabrowski, Liq. Cryst. **26**, 437 (1999).
[16] A. G. Chmielewski, Mol. Chyst. Liq. Cryst. **132**, 339 (1986).
[17] I. S. Berezin and N. P. Zhidkov, Computing Methods, 4th ed. (Pergamon Press, Oxford, 1965).
[18] I. W. Stewart, The Static and Dynamic Continuum Theory of Liquid Crystals. Taylor and Francis, London, 2004.